Electronic Supplementary Material (ESI) for Materials Advances.

EtOH/H_2O Ratio Modulation on Morphology of PFc Carbon for High-V_{oc} (1.03 V) Printable Mesoscopic Perovskite Solar Cells

Jie Sheng‡, Xiaotian Zhu‡, Xiaoli Xu, Jingshan He, Dun Ma, Jialing Liu, Wenjun Wu*

Key Laboratory for Advanced Materials, Feringa Nobel Prize Scientist Joint Research Center, Shanghai Key Laboratory of Functional Materials Chemistry, School of Chemistry and Molecular Engineering, East China University of Science & Technology, 130 Meilong Road, Shanghai 200237, P. R. China

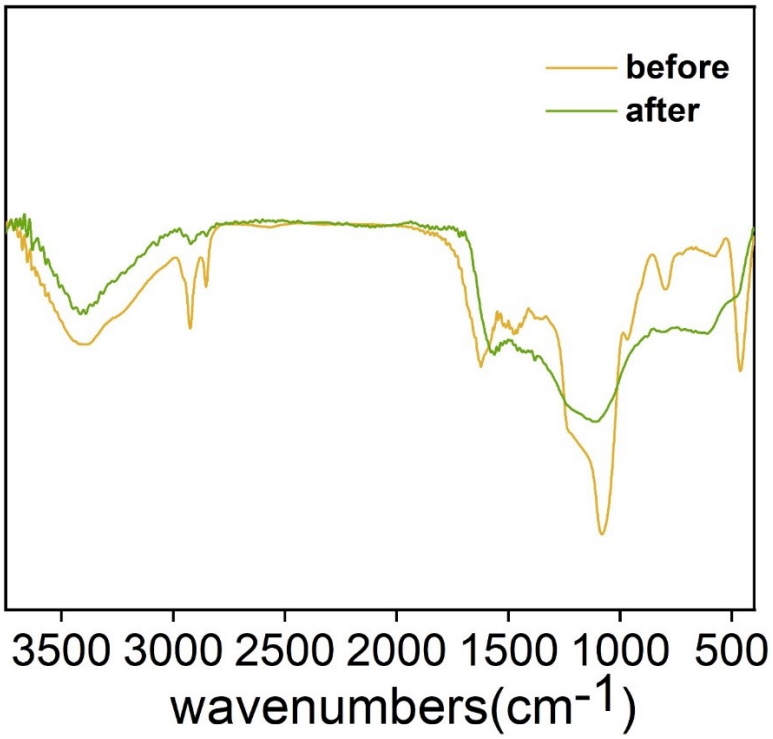

Fig S1. FTIR spectra before and after carbonization.

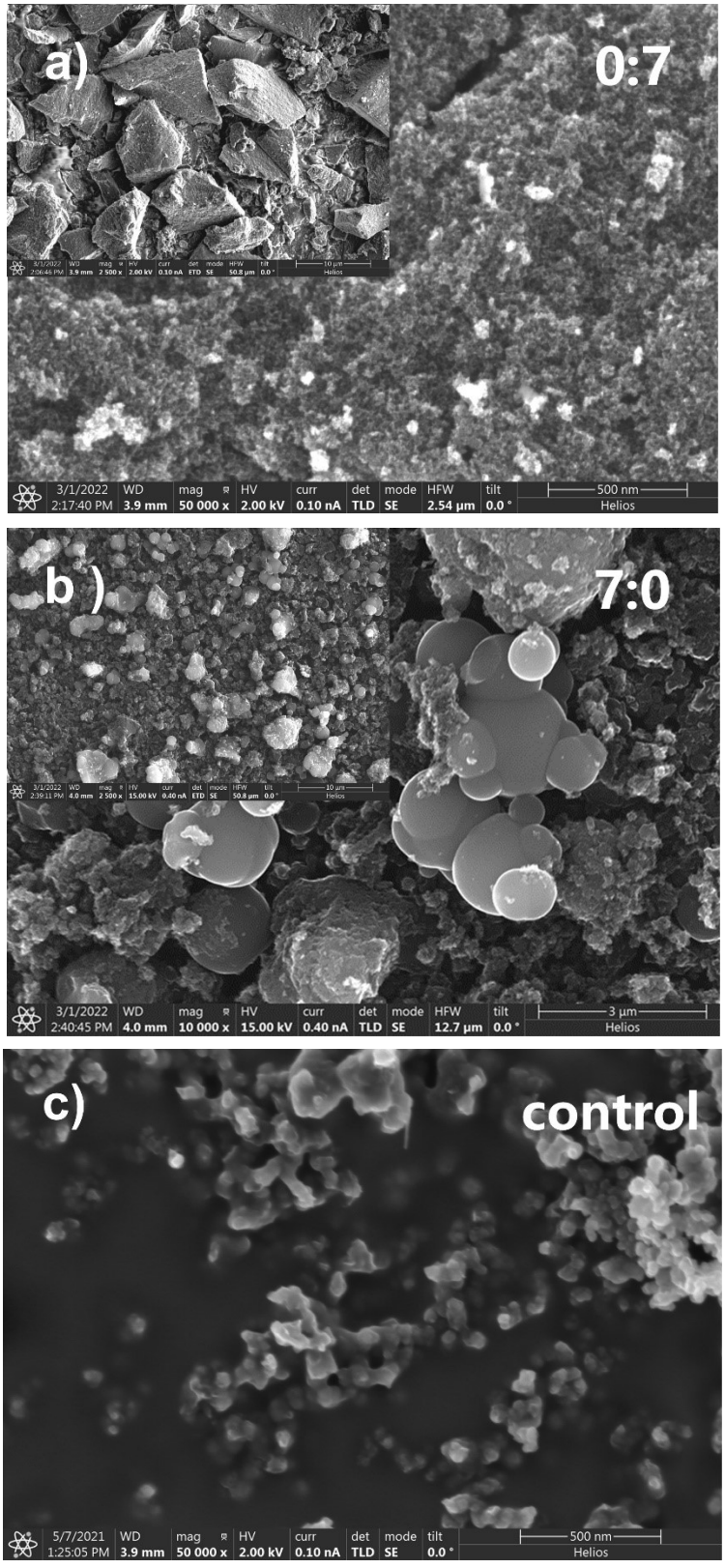

Fig S2. SEM image of a) PFC-0 (ethanol:water = 0:7), b) PFc-7(ethanol:water = 0:7) and c) plain carbon black

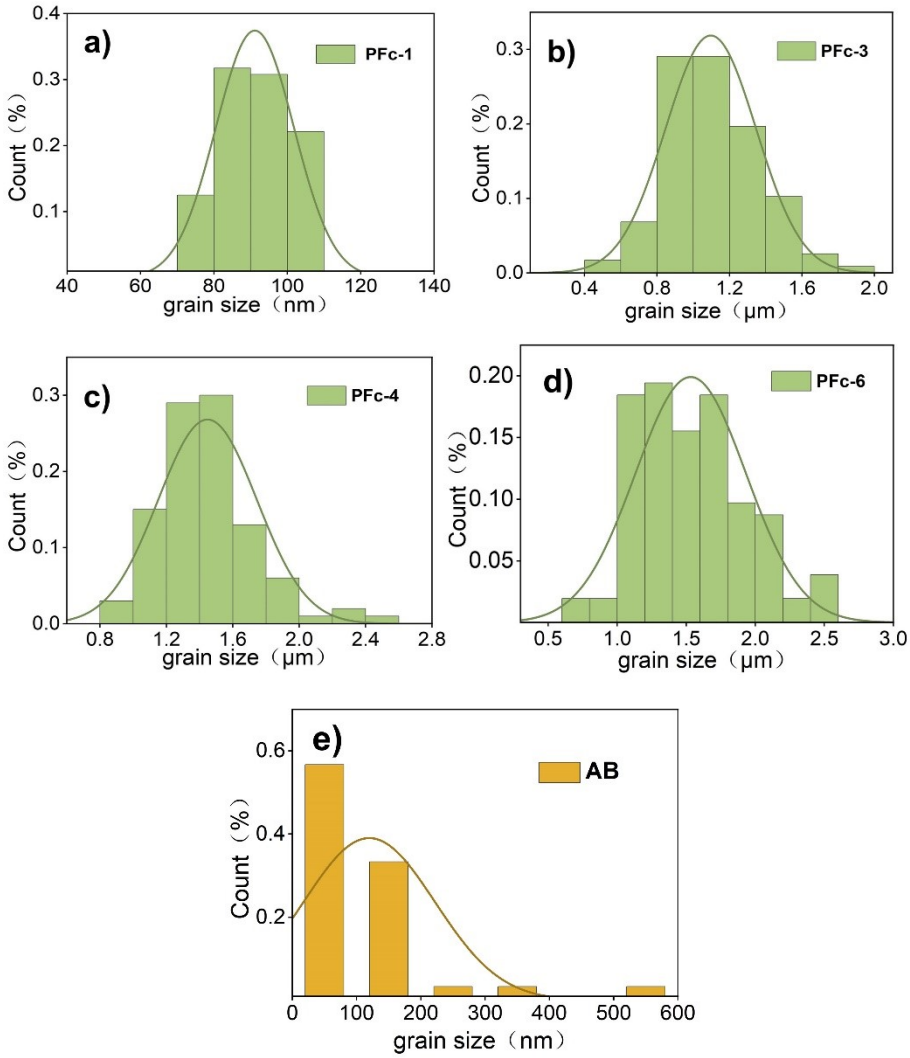

Fig S3. particle size distribution of a) PFc-1, b) PFc-3, c) PFc-4, d) PFc-6, e) plain carbon black.

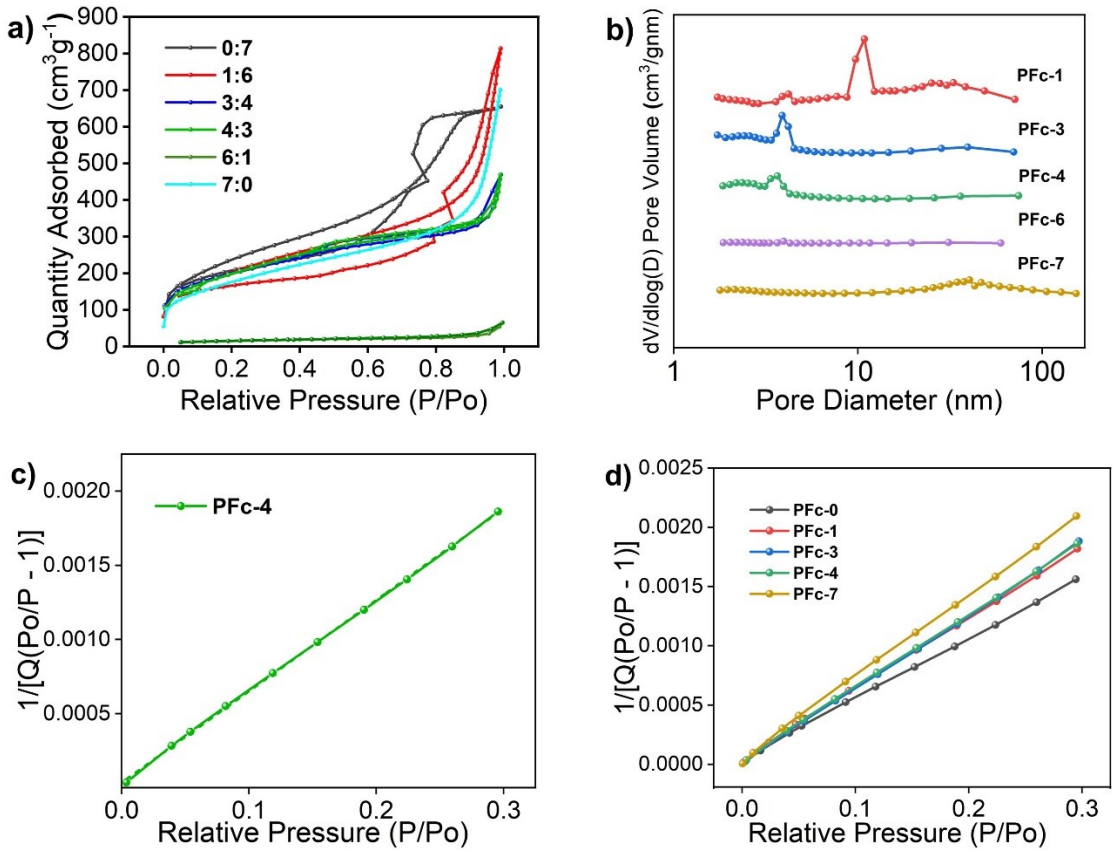

Fig S4. (a) Nitrogen adsorption/desorption isotherms, (b) pore size distribution and (c-d) sorption isotherm of PFc-0, PFc-1, PFc-3, PFc-4, PFc-6, PFc-7.

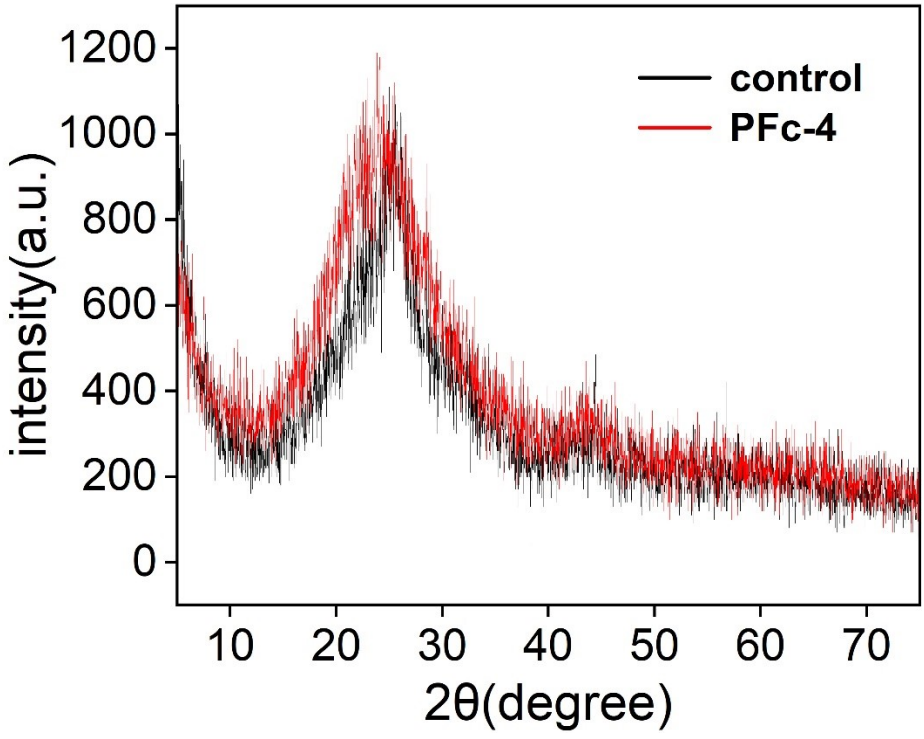

Fig S5. X-ray diffraction (XRD) spectra of PFc-4 and plain carbon black powder

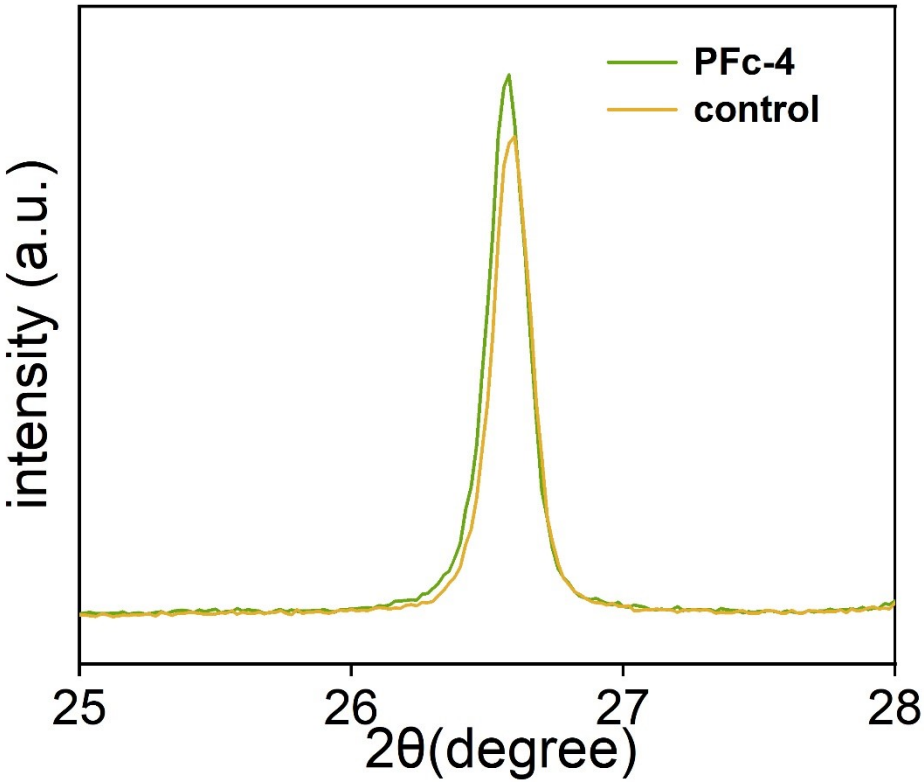

Fig S6. X-ray diffraction (XRD) spectra of PFc-4 and plain carbon black Carbon paste.

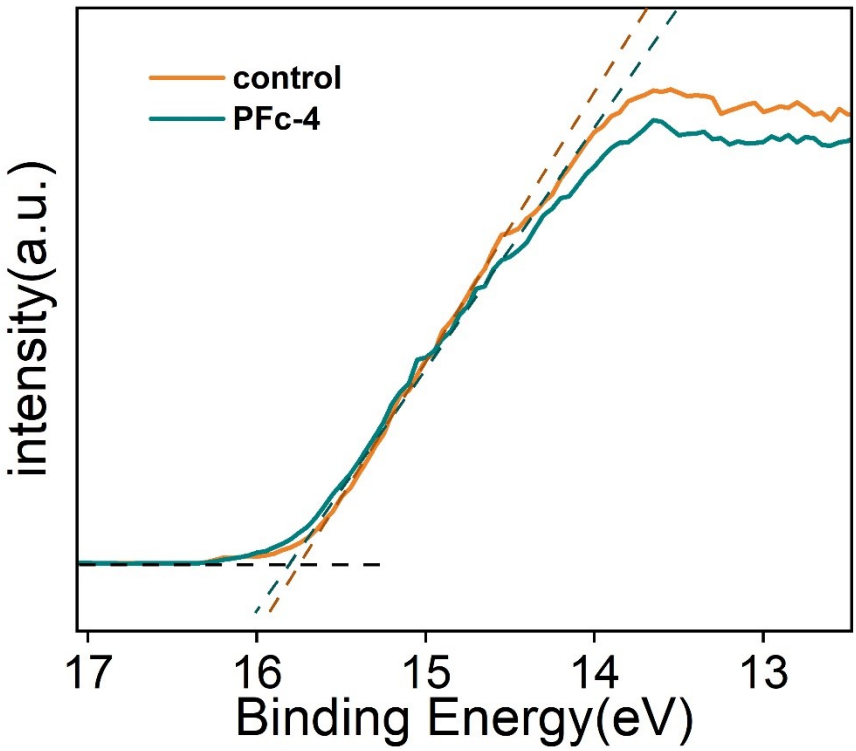

Fig S7. The UPS spectra of the PFc-4 and plain carbon black Carbon paste on FTO glass.

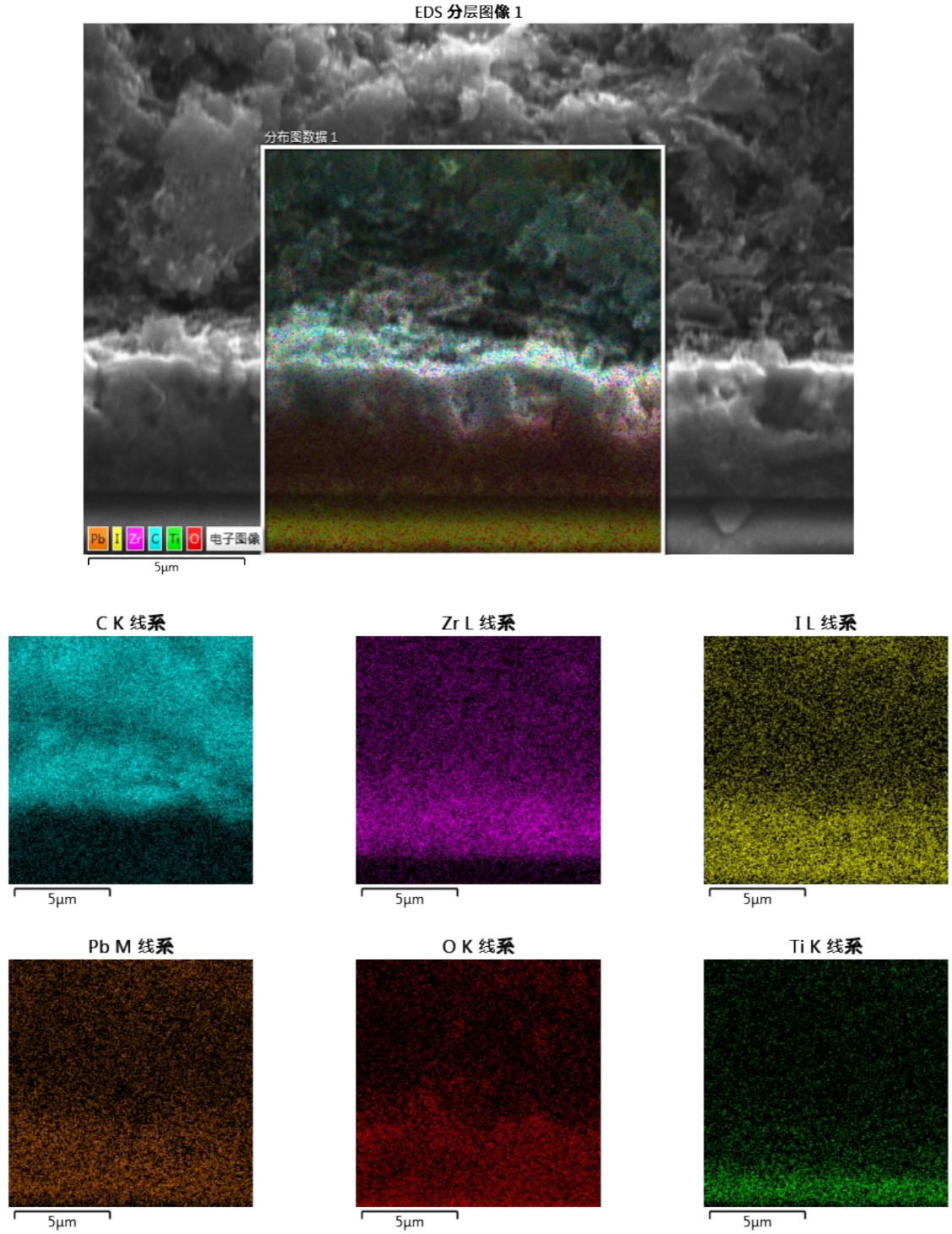

Fig S8. Morphology and energy-dispersive X-ray spectroscopy (EDS) mapping images of p-MPSCs.

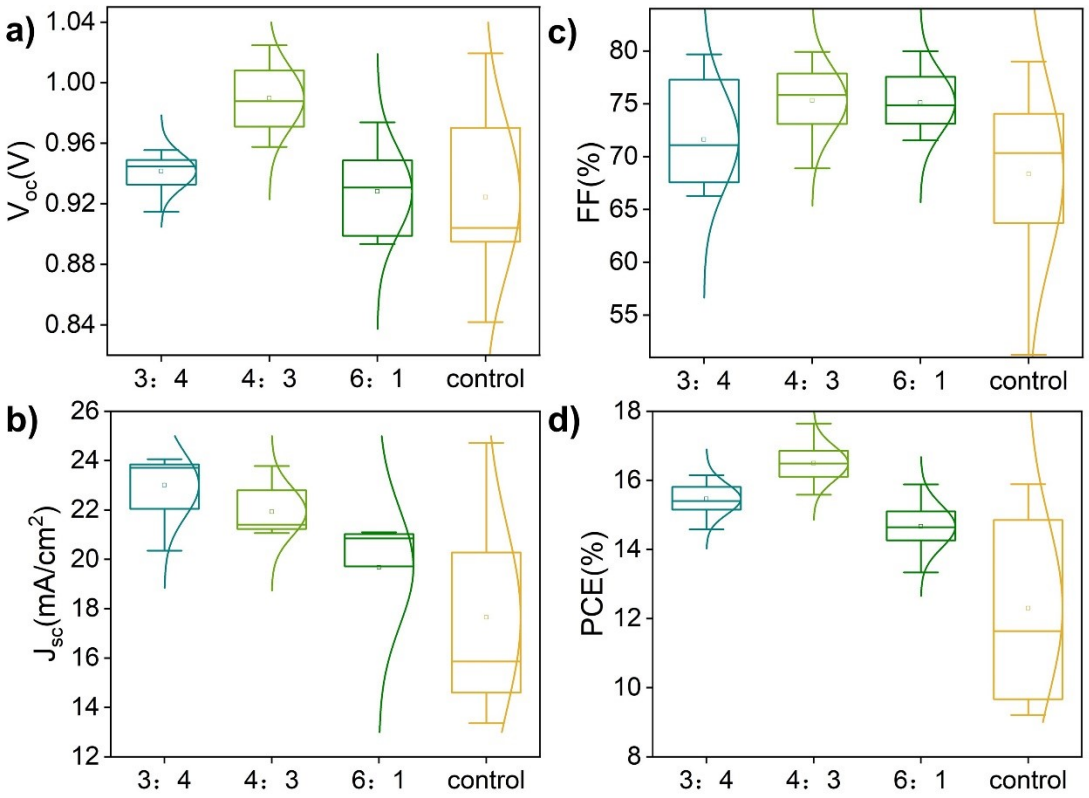

Fig S9. The statistical distribution of Voc, Jsc, FF, and PCE for the devices.

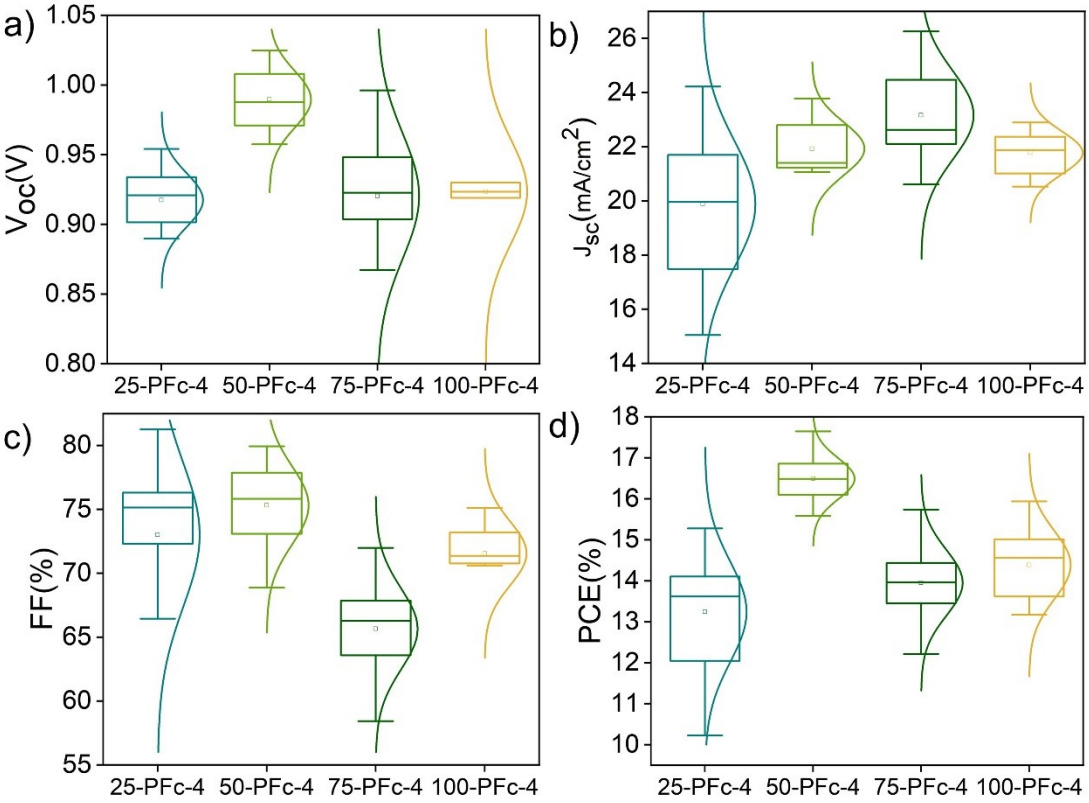

Fig S10. The statistical distribution of Voc, Jsc, FF, and PCE for the devices.

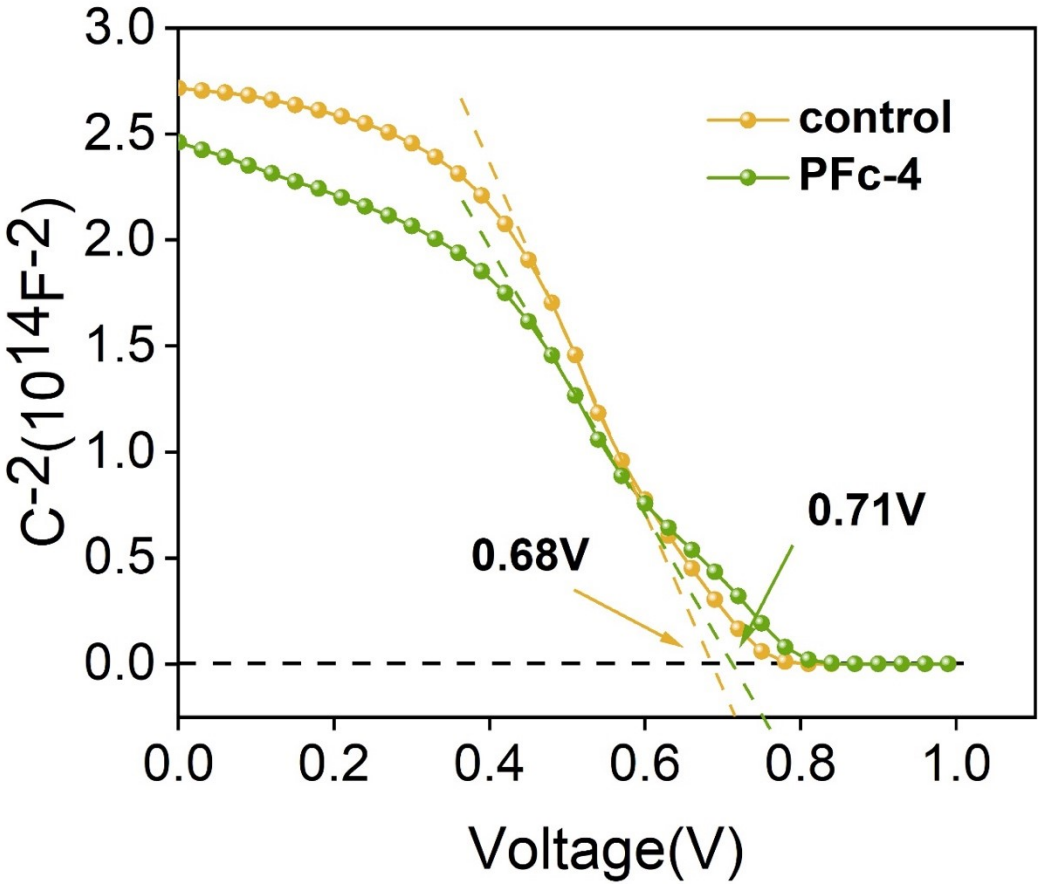

Fig S11. The Mott–Schottky analysis was measured for control and target devices.

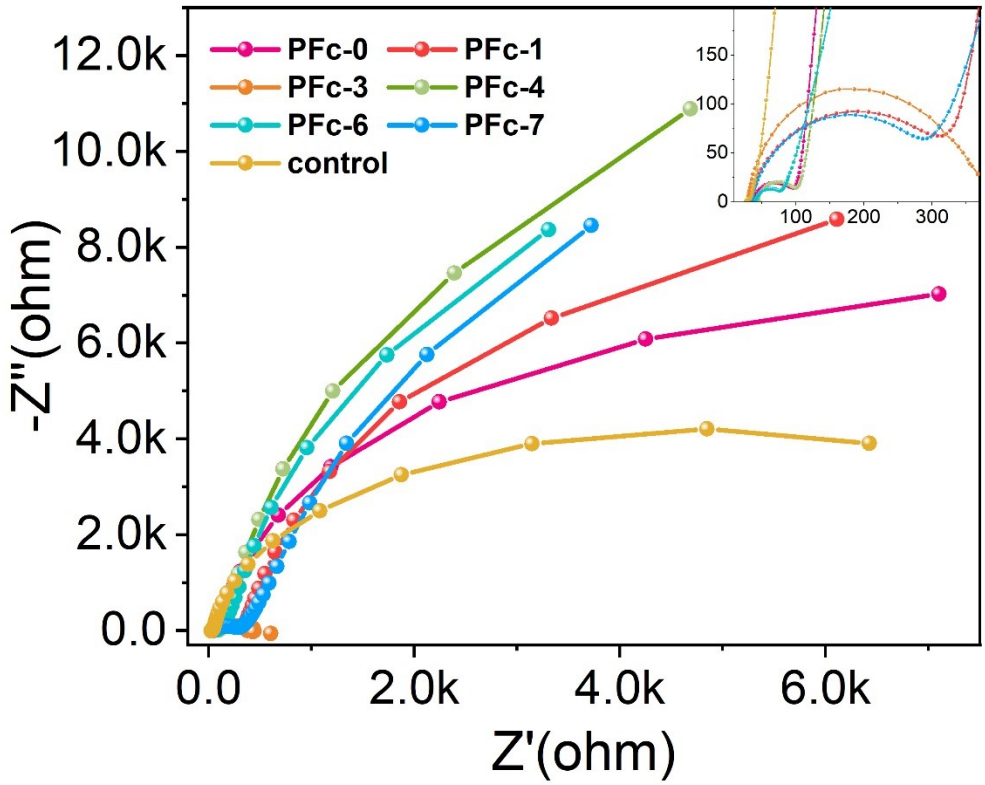

Fig S12. Nyquist plots of PSCs based on control and PFc-x modified p-MPSCs under various values of bias in the dark.

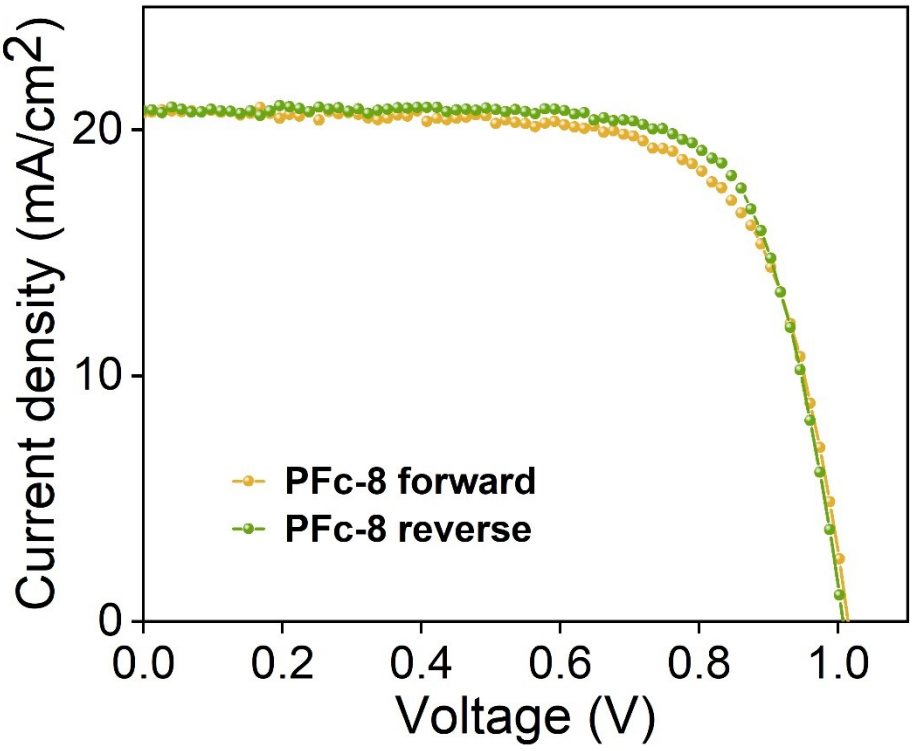

Fig S13 J-V curves of device with PFc-4 under reverse and forward scan.

Table S1. XPS C peak separation results before and after carbonization of PFc-4

Before	Binding energy	Peak area	Ratio	After	Binding energy	Peak area	Ratio
C1	284.79	155085.1	76.96%	C1	284.7299	142669.4	46%
C2	286.28	43256.28	21.47%	C2	285.41	115804.8	37%
C3	288.3323	3166.804	1.57%	C3	288.03	33501.11	11%
C4	293.3719	0.1	0%	C4	291.09	16874.15	5%

C1 = graphitic C, C2 = C-O/C-N, C3 = C=O, C4 = π-π*

Table S2. XPS O peak separation results before and after carbonization of PFc-4

Before	Binding energy	Peak area	Ratio	After	Binding energy	Peak area	Ratio
O1	531.14	13966.01	18%	O1	531.17	10431.92	28%
O2	532.62	64025.02	82%	O2	532.68	20886.48	55%
O3				O3	534.97	3606.661	10%
O4				O4	537	2728.75	7%

O1 = C=O, O2 = C-OH, O3 = COO, O4 = H_2O/occluded CO_2

Table S3. XPS N peak separation results before and after carbonization of PFc-4

Before	Binding energy	Peak area	Ratio	After	Binding energy	Peak area	Ratio
N1	399.2	14082.16	37%	N1	398.3	3822.654	13%
N2	399.9	13543.25	35%	N2	399.8	3436.523	12%
N3	401.5	6824.793	18%	N3	401	11993.93	42%
N4	402.79	3712.118	10%	N4	402.79	9087.494	32%

N1 = $PhNH_2$/N-6, N_2 = N-5, N3 = N-Q, N4 = N-X

Table S4. XPS on the element distribution of PFc-4 before and after carbonization.

Before	Atomic %	After	Atomic %
C1s	79.56	C1s	90.55

N1s	8.38	N1s	4.88
O1s	12.06	O1s	4.57

Table S5. Square resistance of different carbon film

Carbon film	Rsq1（Ω）	Rsq2（Ω）	Rsq3（Ω）	Rsq4（Ω）	Rsq5（Ω）	Mean Rsq（Ω）
PFc-1	12.1	12.1	11.1	11.3	12	11.72
PFc-3	19.6	19.2	18.7	19.7	20	19.44
PFc-4	15.8 16.7	16.1 19.1	17 17.4	17.2 17.2	16.7 17.5	16.57
PFc-6	19	18.9	20.3	18.7	18.1	19
control	18.8	20.9	17.1	18	18.1	18.58

Table S6. Porosity Parameters of mixed solvents with different polarity

Ethanol/water	Samples	S_{BET} (m^2 g^{-1})	Pore volume (cm^3 g^{-1})	Adsorption average pore width(nm)
0:7	PFc-0	839.2227	1.012891	4.82776
1:6	PFc-1	963.8205	1.309419	5.43428
3:4	PFc-3	699.948	0.585404	3.34541
4:3	PFc-4	703.6356	0.589686	3.35223
6:1	PFc-6	55.4431	0.083687	6.03772
7:0	PFc-7	622.8064	0.84285	5.41324

Table S7. Time-resolved PL lifetimes from the biexponential decay model in insulation surface

Insulation surface	A1(%)	τ1(ns)	A2(%)	τ2(ns)	τave(ns)
control	4211.4	7.64	99.64	76.83	15.31
PFc-4	4.97	2.19	141.13	90.31	90.05

Table S8. Time-resolved PL lifetimes from the three exponential decay modes in conductive surface

Conductive surface	A1(%)	τ1(ns)	A2(%)	τ2(ns)	A3(%)	τ3(ns)	τave(ns)
control	13.85	161.82	19.01	152.68	20.57	152.42	155.06
PFc-4	20.05	76.56	16.93	76.56	13.82	76.53	76.55